

1-13-2009

High temperature phases in the $0.98\text{PbZrO}_3-0.02\text{Pb}(\text{Ni}_{1/3}\text{Nb}_{2/3})\text{O}_3$ ceramic

W. Qu

Iowa State University

Xiaoli Tan

Iowa State University, xtan@iastate.edu

N. Vittayakorn

King Mongkut's Institute of Technology

S. Wirunchit

King Mongkut's Institute of Technology

Matthew F. Besser

Iowa State University, besser@ameslab.gov

Follow this and additional works at: http://lib.dr.iastate.edu/mse_pubs



Part of the [Ceramic Materials Commons](#), and the [Physical Chemistry Commons](#)

The complete bibliographic information for this item can be found at http://lib.dr.iastate.edu/mse_pubs/28. For information on how to cite this item, please visit <http://lib.dr.iastate.edu/howtocite.html>.

High temperature phases in the $0.98\text{PbZrO}_3\text{--}0.02\text{Pb}(\text{Ni}_{1/3}\text{Nb}_{2/3})\text{O}_3$ ceramic

Abstract

The phase evolution with temperature in the $0.98\text{PbZrO}_3\text{--}0.02\text{Pb}(\text{Ni}_{1/3}\text{Nb}_{2/3})\text{O}_3$ ceramic was investigated with dielectric permittivity and polarization measurements, hot stage transmission electron microscopy, and high temperature x-ray diffraction. Below 190 °C, the ceramic is in the antiferroelectric phase with characteristic $14\{110\}$ superlattice diffractions. In this stage, typical antiferroelectric 180° domains were observed. Between 190 and 220 °C, an intermediate phase, which is characterized by $12\{110\}$ c-type superlattice diffractions, was detected. Evidences are found to suggest that this intermediate phase is ferroelectric. The $12\{110\}$ c-type superlattice diffraction persists even into the paraelectric phase above 220 °C. In addition, there exists an incommensurate phase between the low temperature antiferroelectric phase and the intermediate ferroelectric phase.

Keywords

Ames Laboratory, Ceramics, Superlattices, X-ray diffraction, Dielectrics, Permittivity, Transmission electron microscopy, Ferroelectric phase transitions, Polarization, Electrical hysteresis, Phase transitions

Disciplines

Ceramic Materials | Materials Science and Engineering | Physical Chemistry

Comments

The following article appeared in *Journal of Applied Physics* 105 (2009): 014106 and may be found at <http://dx.doi.org/10.1063/1.3065087>.

Rights

Copyright 2009 American Institute of Physics. This article may be downloaded for personal use only. Any other use requires prior permission of the author and the American Institute of Physics.



High temperature phases in the 0.98 PbZrO₃ – 0.02 Pb (Ni 1 / 3 Nb 2 / 3) O₃ ceramic

W. Qu, X. Tan, N. Vittayakorn, S. Wirunchit, and M. F. Besser

Citation: *Journal of Applied Physics* **105**, 014106 (2009); doi: 10.1063/1.3065087

View online: <http://dx.doi.org/10.1063/1.3065087>

View Table of Contents: <http://scitation.aip.org/content/aip/journal/jap/105/1?ver=pdfcov>

Published by the [AIP Publishing](#)



Re-register for Table of Content Alerts

Create a profile.



Sign up today!



High temperature phases in the 0.98PbZrO₃–0.02Pb(Ni_{1/3}Nb_{2/3})O₃ ceramicW. Qu,¹ X. Tan,^{1,a)} N. Vittayakorn,² S. Wirunchit,² and M. F. Besser³¹Department of Materials Science and Engineering, Iowa State University, Ames, Iowa 50011, USA²Department of Chemistry, King Mongkut's Institute of Technology, Ladkrabang, Bangkok 10502, Thailand³Materials and Engineering Physics Program, Ames Laboratory, U.S.-DOE, Ames, Iowa 50011, USA

(Received 28 September 2008; accepted 22 November 2008; published online 13 January 2009)

The phase evolution with temperature in the 0.98PbZrO₃–0.02Pb(Ni_{1/3}Nb_{2/3})O₃ ceramic was investigated with dielectric permittivity and polarization measurements, hot stage transmission electron microscopy, and high temperature x-ray diffraction. Below 190 °C, the ceramic is in the antiferroelectric phase with characteristic $\frac{1}{4}\{110\}_c$ superlattice diffractions. In this stage, typical antiferroelectric 180° domains were observed. Between 190 and 220 °C, an intermediate phase, which is characterized by $\frac{1}{2}\{110\}_c$ -type superlattice diffractions, was detected. Evidences are found to suggest that this intermediate phase is ferroelectric. The $\frac{1}{2}\{110\}_c$ -type superlattice diffraction persists even into the paraelectric phase above 220 °C. In addition, there exists an incommensurate phase between the low temperature antiferroelectric phase and the intermediate ferroelectric phase.

© 2009 American Institute of Physics. [DOI: 10.1063/1.3065087]

I. INTRODUCTION

The classic antiferroelectric (AFE) compound lead zirconate (PbZrO₃ or PZ) has been extensively studied since 1950s.¹ At temperatures below 220 °C, PbZrO₃ displays an orthorhombic perovskite structure with antiparallel shifts of Pb²⁺ ions along the pseudocubic $\langle 110 \rangle$ direction, which leads to the AFE behavior.^{1,2} The space group for the low temperature AFE phase was determined to be *Pbam*.^{3–5} At temperatures above 230 °C, PbZrO₃ is in the paraelectric phase with the cubic *m3m* symmetry.² In between the AFE and the paraelectric phase within a narrow temperature range, there is an intermediate phase, which is characterized by $\frac{1}{2}\{110\}_c$ -type superlattice diffractions.^{2,5–8} However, the nature of this intermediate phase is still open for debate. Experimental evidence have been found to support either a ferroelectric^{2,6,7} or an AFE^{5,8} phase.

In our previous study, it has been found that by introducing minor amounts (2–6 mol %) of relaxor ferroelectric Pb(Ni_{1/3}Nb_{2/3})O₃ (PNN) into PZ, the temperature range is expanded for an intermediate phase, which is characterized by an evident frequency dispersion in dielectric permittivity. As a consequence, a series of striking phase transitions was revealed by the dielectric measurement.⁹ In the present work, the 0.98PbZrO₃–0.02Pb(Ni_{1/3}Nb_{2/3})O₃ (PZ98-PNN2) ceramic was selected to further investigate the phase evolution sequence during heating up to 300 °C with hot stage transmission electron microscopy (TEM) and high temperature x-ray diffraction (XRD).

II. EXPERIMENTAL PROCEDURE

The phase pure PZ98-PNN2 ceramic was prepared using the columbite precursor method in order to avoid the pyrochlore phase formation. Detailed preparation procedures have been reported in our previous publications.^{9–11} The rela-

tive density of the as-sintered ceramic was measured using the Archimedes method to be 98%. The grain size was examined by scanning electron microscopy (SEM) (JEOL JSM-606LV). As shown in Fig. 1, the freshly fractured cross section of the PZ98-PNN2 ceramic is almost free of pores and the grain size is in the range of 2–5 μm.

The surface layers of the sintered pellets were removed by mechanical grinding. XRD analysis was performed with Cu *Kα* radiation at a series of temperatures up to 300 °C on a PANalytical X-Pert Pro diffraction system to investigate the structural evolution. Dielectric properties were measured with an LCR meter (HP-4284A, Hewlett-Packard) on a Au-electroded specimen during heating from room temperature to 300 °C at a rate of 2 °C/min. The electrical polarization versus field hysteresis loops were recorded at a series of temperature with a standardized ferroelectric test system (RT-66A, Radiant Technologies). The peak field was maintained at 20 kV/cm during measurement.

Thin disks with a diameter of 3 mm were cut from the as-sintered ceramic pellet, ground, and polished to a thickness of 0.15 mm for TEM specimen preparation. The central portion of the disks was further thinned and polished by mechanical dimpling. Argon ion mill was then used to per-

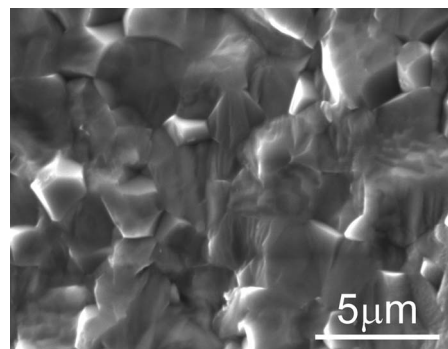


FIG. 1. SEM micrograph of the freshly fractured cross section of the PZ98-PNN2 ceramic.

a)Electronic mail: xtan@iastate.edu.

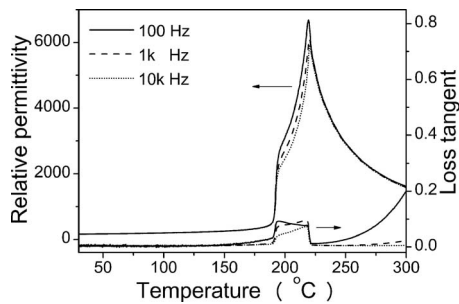


FIG. 2. Dielectric properties during heating at 100 Hz, 1 kHz, and 10 kHz in a bulk PZ98-PNN2 ceramic.

forate the disk at the center. Hot-stage TEM observations were performed with a heating rate less than $2\text{ }^{\circ}\text{C}/\text{min}$ on a Philips CM30 instrument operating at 300 kV. Bright field images and selected area electron diffraction (SAED) patterns were recorded 10 min after the temperature was stabilized.

III. RESULTS AND DISCUSSION

A. Electrical properties

The temperature dependence of relative dielectric permittivity and loss tangent was measured at frequencies of 100 Hz, 1 kHz, and 10 kHz during heating from 30 to $300\text{ }^{\circ}\text{C}$ and the results are displayed in Fig. 2. Clearly, there are two abrupt changes in both relative permittivity and loss tangent in the PZ98-PNN2 ceramic. The first one occurred at around $190\text{ }^{\circ}\text{C}$ where both relative permittivity and loss tangent increased by one order of magnitude. The second abrupt change took place at the Curie temperature of $220\text{ }^{\circ}\text{C}$ where significant suppression of loss tangent is seen. Therefore, the dielectric response in the PZ98-PNN2 ceramic can be divided into three stages. At temperatures below $190\text{ }^{\circ}\text{C}$, the relative permittivity and the loss tangent both have low values and show negligible increases with increasing temperatures. At temperatures above $220\text{ }^{\circ}\text{C}$, the relative permittivity starts to decrease following the Curie-Weiss law, $\epsilon_r = C/(T - T_0)$, where ϵ_r is the relative permittivity, T is the temperature, and C and T_0 are Curie constant and Curie point, respectively. By fitting the data between 220 and $300\text{ }^{\circ}\text{C}$ in Fig. 2, C and T_0 were determined to be 1.89×10^5 and $185.8\text{ }^{\circ}\text{C}$, respectively. In the intermediate temperature range (190 – $220\text{ }^{\circ}\text{C}$), the relative permittivity increases dramatically, while the loss tangent remains high around 0.1. The most remarkable feature of the dielectric behavior in this temperature range is the evident frequency dispersion of both relative permittivity and loss tangent, resembling that in relaxor ferroelectric ceramics. T_{max} , the temperature at which the maximum dielectric permittivity is achieved, was measured to be $219.4\text{ }^{\circ}\text{C}$ at 100 Hz, $220.1\text{ }^{\circ}\text{C}$ at 1 kHz, and $220.4\text{ }^{\circ}\text{C}$ at 10 kHz, respectively, shifting slightly toward higher temperatures with increasing frequency.

To further clarify the dielectric behavior of the different phases in the PZ98-PNN2 ceramic, electrical polarization hysteresis loop measurements were performed under a peak field of 20 kV/cm at a series of temperatures. During heating,

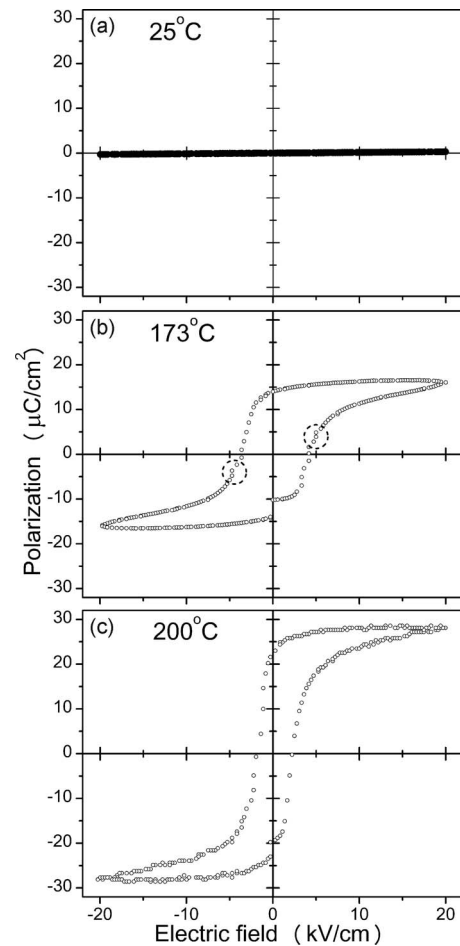


FIG. 3. Polarization hysteresis loops recorded from a bulk PZ98-PNN2 ceramic at 4 Hz during heating at (a) $25\text{ }^{\circ}\text{C}$, (b) $173\text{ }^{\circ}\text{C}$, and (c) $200\text{ }^{\circ}\text{C}$.

the two electrodes were shortened. The loop was recorded after the temperature was stabilized for at least 5 min. As shown in Fig. 3(a), very small polarizations can be induced by the applied electric field in the ceramic at room temperature. This is typical for an AFE ceramic subjected to electric fields that are not sufficient to induce the AFE to ferroelectric phase transition. Such a linear behavior with minimum polarization remains at temperatures up to $170\text{ }^{\circ}\text{C}$.

When the temperature further increases, a hysteretic behavior starts to develop. As shown in Fig. 3(b), a regular hysteresis loop with a coercive field E_c of 3.9 kV/cm was recorded at $173\text{ }^{\circ}\text{C}$. However, the observed hysteresis loop does not indicate the presence of a ferroelectric phase. Close examination of the loop in Fig. 3(b) reveals that slight distortions occurred at $\sim 5\text{ kV/cm}$, marked with the two dashed circles on the hysteresis loop. Similar distortions on hysteresis loops were found in $\text{Pb}_{0.99}\text{Nb}_{0.02}[(\text{Zr}_{0.57}\text{Sn}_{0.43})_{1-y}\text{Ti}_y]_{0.98}\text{O}_3$ ceramics and have been attributed to the onset of the electric field-induced AFE to ferroelectric phase transition.¹² Therefore, the PZ98-PNN2 ceramic at this temperature is still in the AFE phase. It should be noted that the distortions marked in Fig. 3(b) indicate the AFE-to-ferroelectric phase transition. The distortion associated with the backward ferroelectric-to-AFE transition was not seen because it may overlap with the coercive field of the induced ferroelectric phase. The observed large

polarization is due to the induced ferroelectric phase by the applied field of 20 kV/cm, which is much higher than the critical electric field E_F of ~ 5 kV/cm.

Further increase in temperature leads to the decrease in the critical field E_F and the increase in both the saturation polarization P_s and the remanent polarization P_r . P_r saturates at $25 \mu\text{C}/\text{cm}^2$ when the temperature reaches 177°C and stays unchanged up to 186°C . It should be noted that the coercive field E_c (not the critical field E_F) remains the same at 3.9 kV/cm in the temperature range of 172 – 186°C . The results suggest that the volume fraction of the ferroelectric phase induced by a field of 20 kV/cm in the ceramic increases with increasing temperatures between 172 and 177°C . In the temperature range of 177 – 186°C , the whole piece of sample was forced into a ferroelectric phase by the external electric field of 20 kV/cm. Therefore, the P_r saturates in this temperature range.

Dramatic change in the coercive field E_c was observed at 186°C . At this temperature, although a well defined hysteresis loop was still observed, E_c abruptly reduced to 2.4 kV/cm, indicating the appearance of a new phase. Up to 200°C , the hysteresis loop remains largely unchanged, with the one at 200°C shown in Fig. 3(c).

Combined with the results presented in Fig. 2, we believe that the abrupt change in E_c at 186°C marks the phase transition at 190°C revealed by the dielectric measurement. The discrepancy in temperature is due to the different test conditions. In the dielectric measurement, the ceramic sample was subjected to continuous heating at a rate of $2^\circ\text{C}/\text{min}$, while in the polarization measurement, the hysteresis loops were recorded after at least 5 min the temperature is stabilized. In summary, the macroscopic property measurements reveal that at temperatures below 190°C , the PZ98-PNN2 ceramic is AFE with stable and low dielectric permittivity and loss tangent. Under applied electric fields, the AFE phase can be transformed into a ferroelectric phase at temperatures slightly below the transition temperature. An intermediate phase exists between 190 and 220°C . The increased loss tangent and the well defined hysteresis loops with reduced coercive fields E_c seem to suggest that this phase is ferroelectric.² Further supporting evidence is found in our previous study where the intermediate phase is stabilized down below room temperature in the PZ90-PNN10 ceramic and an undistorted hysteresis loop was observed in this ceramic at room temperature.¹⁰ However, this intermediate phase is a unique ferroelectric phase with evident frequency dispersion in its dielectric behavior.

B. Hot stage TEM

The temperature induced phase transitions were visualized by hot stage TEM during heating. One grain about $3 \mu\text{m}$ in size was tilted so that its $\langle 001 \rangle$ -zone axis was aligned with the electron beam direction. The evolution of the SAED pattern with temperature is exemplified in Fig. 4. At room temperature, the primary feature is the presence of the $\frac{1}{4}\{110\}_c$ -type superlattice diffraction spots [Fig. 4(a)], where the subscript c indicates that the indices are based on the parent cubic perovskite unit cell. The superlattice struc-

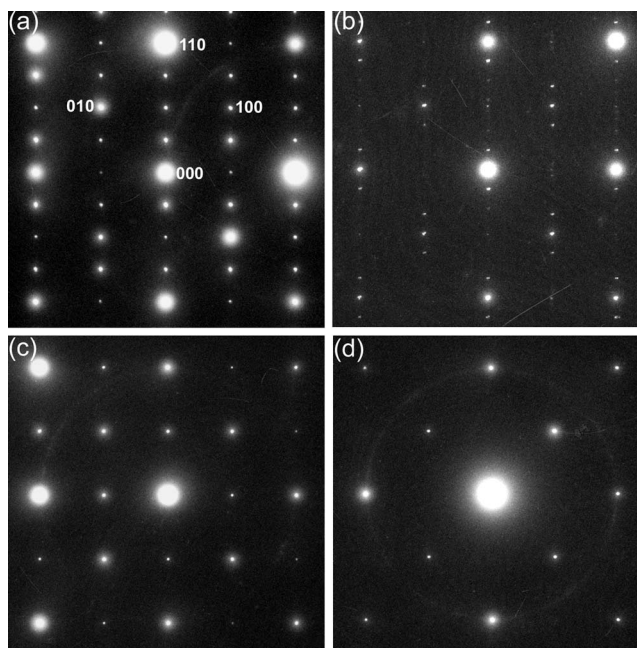


FIG. 4. Hot stage *in situ* TEM experiment on a thin foil specimen of the PZ98-PNN2 ceramic. The $\langle 001 \rangle_c$ -zone axis SAED patterns observed during heating at (a) 25°C , (b) 179°C , (c) 194°C , and (d) 240°C .

ture is identical to that of PbZrO_3 at room temperature.^{2,6,7} Therefore, adding 2 mol % of PNN does not change the crystal structure of PbZrO_3 . The SAED pattern with the $\frac{1}{4}\{110\}_c$ superlattice spots does not change with increasing temperature up to 179°C .

At 179°C , the $\frac{1}{4}\{110\}_c$ superlattice spots disappeared, as shown in Fig. 4(b). Instead, incommensurate superlattice diffraction spots emerged. These extra diffraction spots are of the $\frac{1}{n}\{110\}_c$ -type, where n is not an integer. The value of n is determined to be 6.48 for the PZ98-PNN2 ceramic from Fig. 4(b). The incommensurate superlattice diffraction spots only existed over a narrow temperature range of $\sim 3^\circ\text{C}$ and completely disappeared at 181°C . This type of incommensurate superlattice diffraction has been previously observed in PbZrO_3 and was attributed to the competition between the low temperature AFE phase and the intermediate ferroelectric phase.⁶

In the temperature range of 181 – 212°C , the primary feature in SAED patterns is the presence of $\frac{1}{2}\{110\}_c$ -type superlattice diffraction, as exemplified by the diffraction pattern recorded at 194°C shown in Fig. 4(c). The $\frac{1}{2}\{110\}_c$ superlattice diffraction was reported previously and has been considered as the signature of the intermediate phase in PbZrO_3 .^{2,5–8} However, considerable controversy remains concerning the symmetry and the nature of the intermediate phase. It was reported to be either rhombohedral⁶ or orthorhombic,^{5,7} either ferroelectric^{2,6,7} or AFE.^{5,8}

The $\frac{1}{2}\{110\}_c$ superlattice diffraction started to become weaker and diffuse at 212°C and finally vanished at 240°C . Further increase in temperature up to 300°C did not lead to any change in the diffraction pattern. The SAED pattern at 240°C is shown in Fig. 4(d) and can be indexed with the parent cubic perovskite structure.

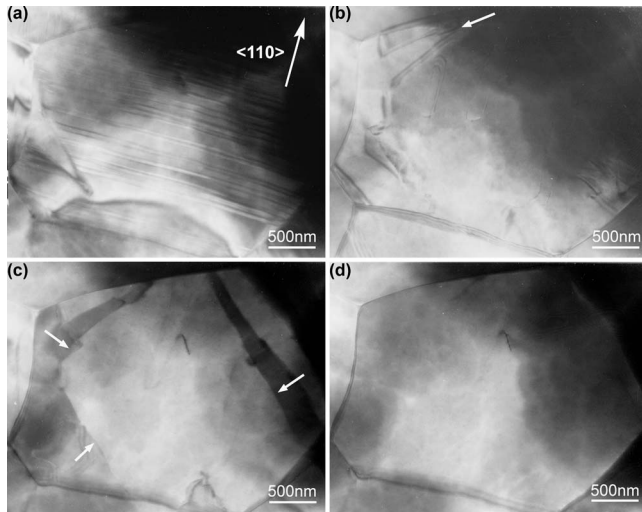


FIG. 5. The bright field micrographs under the $\langle 001 \rangle_c$ -zone axis of the grain used for the electric diffraction study in Fig. 4 at (a) 148 °C, (b) 179 °C, (c) 186 °C, and (d) 300 °C.

Corresponding changes in the bright field image of the same grain were observed as well, as shown in Fig. 5. From room temperature to 179 °C, one set of lamellar 180° AFE domains was observed in the grain [Fig. 5(a)], consistent with the one set of $\frac{1}{4}\{110\}_c$ superlattice spots in the diffraction pattern. These lamellar domains became thinner as temperature was increased. At 179 °C, corresponding to the appearance of the $1/n\{110\}_c$ incommensurate and the disappearance of the $\frac{1}{4}\{110\}_c$ superlattice diffraction, the 180° AFE domains in the whole grain were replaced by wedge-shaped domains near grain boundaries. The tip of one wedge-shaped domain is marked by an arrow in Fig. 5(b). In the temperature range of 181–212 °C, corresponding to the $\frac{1}{2}\{110\}_c$ -type superlattice diffraction in SAED patterns, the grain displays a checkerboard-like domain morphology with domain walls primarily on the $\{100\}_c$ planes. The domain walls of the large domain with bright contrast are indicated by arrows in Fig. 5(c). Such domain morphology is a reminiscence of the AFE domains in lead zirconate stannate titanate ceramics.¹³ The walls of these checkerboard-like domains started to move and disappear at 212 °C and completely vanished at 224 °C. This grain remains contrast free during the further heating up to 300 °C, as shown in Fig. 5(d).

Compared with the results from dielectric measurement in bulk samples, the *in situ* TEM heating experiment reveals almost the same phase transition sequence. Below 179 °C, the PZ98-PNN2 ceramic is in the AFE phase that is isostructural to PbZrO₃. Between 181 and 212 °C, the ceramic is in the intermediate ferroelectric phase characterized by the $\frac{1}{2}\{110\}_c$ -type superlattice diffraction and the checkerboard-like domains. Above 212 °C, the ceramic is in the paraelectric phase. However, the $\frac{1}{2}\{110\}_c$ -type superlattice diffraction and the checkerboard domain morphology persists up to 224 °C in the paraelectric phase. The persistence of the $\frac{1}{2}\{110\}_c$ superlattice into paraelectric phase was noticed before in PbZrO₃.^{2,6} The difference in the transition temperatures between the TEM experiment and the dielectric mea-

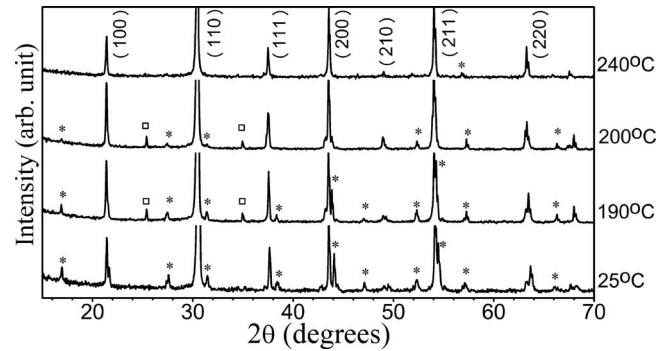


FIG. 6. XRD patterns of a bulk PZ98-PNN2 ceramic during heating at 25, 190, 200, and 240 °C.

surement is due primarily to the different sample geometries. The advantage of the *in situ* TEM study over the dielectric measurement is manifested in the revealing of the transient incommensurate phase around 179 °C between the low temperature AFE phase and the intermediate phase.

C. High temperature XRD

The crystal structure of the PZ98-PNN2 ceramic was further analyzed with XRD at a series of temperatures during the heating process. Four temperatures were selected to record the diffraction pattern: 25 °C where the AFE phase isostructural to PbZrO₃ is expected, 190 °C where the incommensurate phase is expected in the bulk sample, 200 °C where the intermediate phase is expected, and 240 °C where the paraelectric phase should be dominant. All the patterns were recorded after the temperature was stabilized at the desired temperature for at least 10 min. The results are shown in Fig. 6, where the major peaks are indexed based on a cubic unit cell.

At 25 °C, the diffraction pattern fits the space group *Pbam*, the same as PbZrO₃ at room temperature.^{3–5} The peaks marked by the asterisks indicate the peaks that belong to this symmetry but are forbidden in the cubic structure. All these peaks can be indexed as $\frac{1}{4}\{110\}_c$ -type superlattice diffractions. When the temperature increased to 190 °C, orthorhombic *Pbam* symmetry remained, as indicated by the asterisks. However, two additional peaks, one on each side of the $\{110\}_c$ peak, emerged at 25.4° and 35.0°, respectively. They are marked with squares in Fig. 6. These additional peaks cannot be indexed with either cubic or orthorhombic symmetry. Considering the observed incommensurate phase observed in TEM, these two peaks may be the satellite diffraction peaks of the strongest $\{110\}_c$ peak. This is indeed the case. They can be indexed as $\{110\}_c - 1/n\{110\}_c$ and $\{110\}_c + 1/n\{110\}_c$, respectively, with $n=6.48$. This value of n is exactly the same as determined by the TEM result. The observation of the incommensurate modulation with XRD is significant because so far it has been only revealed by electron diffraction in TEM in PbZrO₃-based ceramics.¹⁴

On further heating to 200 °C, the $\frac{1}{4}\{110\}_c$ -type superlattice peaks became weaker and some of them even disappeared. While an orthorhombic symmetry was reserved, the overall pattern fits better with the space group *P2cb*. To our surprise, the incommensurate superlattice peaks can still be

clearly observed. This appears to disagree with the TEM result shown in Fig. 4, where the incommensurate satellite spots existed over a very narrow temperature range of less than 3 °C. This discrepancy can be explained by considering the difference in the experimental conditions. In the TEM experiment, observations were made in a single grain, while in XRD, hundreds of thousands of grains were exposed to the x-ray beam. The unsynergized phase transition of each individual grain leads to a much wider temperature range for the incommensurate phase.

At 240 °C where the PZ98-PNN2 ceramic is supposed to be in the high temperature paraelectric phase, the major peaks can be indexed with a cubic symmetry. However, close examination revealed the presence of trace amount of the orthorhombic phase.

IV. CONCLUSIONS

By introducing 2 mol % $\text{Pb}(\text{Ni}_{1/3}\text{Nb}_{2/3})\text{O}_3$ into PbZrO_3 , a series of phase transitions occurred above room temperature. The high temperature phases show distinct crystal structures and domain morphologies, as well as distinct dielectric and ferroelectric properties. Below 190 °C, the ceramic is in the *Pbam* symmetry with AFE 180° domains. Both the dielectric permittivity and the loss tangent are low and stable against temperature change. Around 190 °C, one order of magnitude increase in dielectric permittivity and loss tangent occurs within a narrow temperature range. Corresponding to the dramatic change in dielectric property is the presence of an incommensurate phase with $\frac{1}{6.48}\{110\}_c$ satellite diffractions. In the temperature range of 190–220 °C, the ceramic is in an intermediate phase, which is believed to be ferroelectric. This phase is characterized by the fast increasing dielectric permittivity, stable and high loss tangent, well defined polarization hysteresis loops, and the $\frac{1}{2}\{110\}_c$ superlattice diffraction. This ferroelectric intermediate phase is unique

because of the frequency dispersion in its dielectric properties, the checkerboard-like morphology of its domain structure, and the orthorhombic space group of *P2cb*. Above 220 °C, the ceramic is in the cubic paraelectric phase with the relative permittivity following the Curie–Weiss law. However, the structural change at the Curie point is by no means abrupt. Some residual orthorhombic phase persists even at temperatures several tens of degrees above 220 °C.

ACKNOWLEDGMENTS

This work was supported by the National Science Foundation through the CAREER Grant No. DMR-0346819 and the U.S.–Israel Binational Science Foundation through Grant No. 2006235. The *in situ* TEM and high temperature XRD experiments were carried out at the Materials & Engineering Physics Program, Ames Laboratory, which is supported by the United States Department of Energy–Basic Energy Sciences under Contract No. DE-AC02-07CH11358.

¹E. Sawaguchi, H. Maniwa, and S. Hoshino, *Phys. Rev.* **83**, 1078 (1951).

²D. Viehland, *Phys. Rev. B* **52**, 778 (1995).

³D. L. Corker, A. M. Glazer, J. Dec, K. Roleder, and R. W. Whatmore, *Acta Crystallogr., Sect. B: Struct. Sci.* **53**, 135 (1997).

⁴K. Yamasaki, Y. Soejima, and K. F. Fischer, *Acta Crystallogr., Sect. B: Struct. Sci.* **54**, 524 (1998).

⁵S. Teslic and T. Egami, *Acta Crystallogr., Sect. B: Struct. Sci.* **54**, 750 (1998).

⁶Z. Xu, X. Dai, D. Viehland, and D. A. Payne, *J. Am. Ceram. Soc.* **78**, 2220 (1995).

⁷M. Tanaka, R. Saito, and K. Tsuzuki, *Jpn. J. Appl. Phys., Part 1* **21**, 291 (1982).

⁸H. Fujishita and S. Hoshino, *J. Phys. Soc. Jpn.* **53**, 226 (1984).

⁹S. Wirunchit and N. Vittayakorn, *J. Appl. Phys.* **104**, 024103 (2008).

¹⁰N. Vittayakorn and S. Wirunchit, *Smart Mater. Struct.* **16**, 851 (2007).

¹¹S. Wirunchit, P. Laoratanakul, and N. Vittayakorn, *J. Phys. D* **41**, 125406 (2008).

¹²H. He and X. Tan, *J. Phys.: Condens. Matter* **19**, 136003 (2007).

¹³H. He and X. Tan, *Phys. Rev. B* **72**, 024102 (2005).

¹⁴J. Ricote, D. L. Corker, R. W. Whatmore, S. A. Impney, A. M. Glazer, J. Dec, and K. Roleder, *J. Phys.: Condens. Matter* **10**, 1767 (1998).